Organic Geochemistry 42 (2011) 640–654

Contents lists available at ScienceDirect

Organic Geochemistry

journal homepage: www.elsevier.com/locate/orggeochem

Hydrocarbon biomarkers of Neoproterozoic to Lower Cambrian oils from eastern Siberia

Amy E. Kelly [a,b,1], Gordon D. Love [b], John E. Zumberge [c], Roger E. Summons [a,*]

[a] Department of Earth, Atmospheric and Planetary Sciences, Massachusetts Institute of Technology, Cambridge, MA 02139, USA
[b] Department of Earth Sciences, University of California, Riverside, CA 92521, USA
[c] GeoMark Research Ltd., Houston, TX 77095, USA

ARTICLE INFO

Article history:
Received 22 September 2010
Received in revised form 20 March 2011
Accepted 28 March 2011
Available online 14 April 2011

ABSTRACT

The Neoproterozoic Era is of widespread geobiological interest because it marks the critical transition from a world of microbes to one where animals become an established feature of the landscape. Much research into this time period has focused on the ventilation of the oceans, as this is widely considered a primary factor driving the diversification of complex, multicellular life. In this study, Proterozoic to Cambrian aged oils from eastern Siberia were analyzed for their hydrocarbon biomarker contents and compound specific carbon isotopes in order to further our understanding of the prevailing environment and its microbial and metazoan communities. Geochemically, these oils are broadly comparable to those of the Ediacaran–Cambrian sedimentary rocks and oils of the South Oman Salt Basin. Organic matter in the source sedimentary rocks included significant contributions from green algae, demosponges and bacteria including cyanobacteria and methanotrophic proteobacteria. Although the ages of the Siberian oils and putative parent source rock intervals are poorly constrained, the geochemical similarities between the Ediacaran Oman Huqf and Nepa-Botuoba-Katanga family of Siberian oil samples are impressive, leading to the inference that their source rocks are coeval. On the other hand, oils from the Baykit High are distinctive, likely older and possibly of Cryogenian age.

1. Introduction

The close of the Proterozoic Eon saw great change in Earth's surface environment and its biota. There were at least two lengthy periods when Earth was extensively glaciated, even at low latitude, widely known as 'Snowball Earth' episodes. These were the Sturtian glaciation terminating around 730–710 Ma and the Marinoan which ended around 635 Ma (Hoffmann et al., 2004; Macdonald et al., 2010). There was also a more regional, short-term event, the Gaskiers glaciation at around 580 Ma (Bowring et al., 2003). Diverse geochemical proxies recorded in marine sedimentary rocks show that the deep ocean basins of the Proterozoic were initially anoxic and, likely, sulfidic in intermediate water depth layers around continental margins and that ventilation began about the time of the Cambrian Explosion (Cloud, 1968; Des Marais et al., 1992; Canfield and Teske, 1996; Canfield, 1998; Anbar and Knoll, 2002; Knoll et al., 2004; Narbonne, 2005; Fike et al., 2006; McFadden et al., 2008; Scott et al., 2008; Dahl et al., 2010; Li et al., 2010).

Toward the end of the Neoproterozoic Era the first macroscopic metazoan body fossils are observed; this is followed by the rapid diversification of modern animal phyla during the Cambrian Period (Knoll and Carroll, 1999). The macroscopic metazoans include the well documented Ediacaran faunal assemblages, acritarchs some of which may represent the remains of animal embryos (Van Waveren and Marcus, 1993; Yin et al., 2004; Knoll et al., 2006) and enigmatic fabrics reported in Cryogenian sediments (Giddings et al., 2009; Maloof et al., 2010) that may also be animal body fossils or, possibly, macroscopic protists. Many forms of geological and geochemical evidence suggest that there were unprecedented and globally significant changes to the biogeochemical cycles of carbon, sulfur and nitrogen, and in distributions of redox sensitive trace elements, taking place throughout this entire interval. The triggers for these environmental transformations, however, remain unclear and subject to intense debate (Logan et al., 1995; Rothman et al., 2003; Peterson and Butterfield, 2005; Kennedy et al., 2006;Bristow and Kennedy, 2008; Derry, 2010).

The goal of this research was to query lipid biomarker proxies for information on organic matter inputs and the paleoenvironmental context of petroleum deposits that originated from Mesoproterozoic-Cambrian sedimentary sequences of eastern Siberia. Here, high abundances of well preserved organic carbon, bitumen and petroleum can be found in sedimentary rocks that have not

* Corresponding author.
E-mail addresses: kellya@alum.mit.edu (A.E. Kelly), glove@ucr.edu (G.D. Love), jzumberge@geomarkresearch.com (J.E. Zumberge), rsummons@mit.edu (R.E. Summons).
[1] Present address: School of Earth and Space Exploration, Arizona State University, Tempe, AZ 85287, USA.

0146-6380/$ - see front matter © 2011 Elsevier Ltd. All rights reserved.
doi:10.1016/j.orggeochem.2011.03.028

experienced high temperatures in the geological past (Hayes et al., 1992; Summons and Powell, 1992). At the same time, we hoped to gain insight into the compositions of the microbial and metazoan communities that proliferated in the paleoenvironments where the petroleum source rocks were deposited.

Petroleum samples were obtained from the Baykit High region ($n = 6$), the Katanga Saddle within the greater Cis-Sayan Basin ($n = 4$), and from the Nepa-Botuoba Basin of the Nepa-Botuoba High region ($n = 15$), as shown in Fig. 1. A composite stratigraphy is shown in Fig. 2 based on our interpretation of parent source rock age from comparison with geochemical characteristics of South Oman sedimentary rocks and oils (see Section 4.4). The Russian stratigraphic nomenclature for this time interval comprises the Riphean (1650–650 Ma), which is roughly the Mesoproterozoic to Middle Neoproterozoic and Vendian (650–542 Ma), which roughly equates to the Ediacaran. In order to be faithful to both the system from which the samples come and the current internationally recognized period names, we use both where appropriate. Further, we infer that Riphean aged oils and their source rocks are from the latest Riphean and thus Cryogenian (850–635 Ma) according to the International Stratigraphic Chart of 2009. Unfortunately, data from specific source rocks in this region are unavailable. However, a recent analysis of eastern Siberian oils, including those from the study area, concludes that all the oils derive from Precambrian source rocks and that the Nepa-Botuoba and Baykit High oils are from distinct petroleum systems (Everett, 2010).

The petroleum habitat of the Baykit High region of eastern Siberia has been reviewed by Ulmishek (2001a) where Riphean System carbonate and clastic strata were deposited on Archean–Lower Proterozoic basement. Basal Vendian (Sokolov and Fedonkin, 1990) clastic sediments unconformably overlie the Riphean rocks and, in some places, the basement directly. These are overlain, in turn, by a sequence of Late Vendian to lowermost Cambrian dolomitic carbonates and evaporites. However, in the absence of robust geochronological data, fossils and good quality seismic data, it is recognized that the many aspects of the stratigraphy and regional geology are inadequately understood (Ulmishek, 2001a). The Baykit petroleum is perceived to represent a single petroleum system reservoired in, and thought to have been sourced from, the older and structurally distinct Riphean sequence. Prospective source rocks have not been identified in the Baykit High stratigraphic section itself. However, organic rich shales and carbonates of late Riphean age have been found in outcrop in the Yenisey Ridge foldbelt west of the Baykit High. Kontorovich and others hypothesized that a thick sequence of organic rich shales of the Shuntar Formation of the Tungusik series (>c. 1050 Ma) is a likely source, given that sediments capable of sourcing petroleum are notably absent from the Vendian section (Kontorovich et al., 1996), but their arguments are based solely on the preponderance of organic matter in stratigraphic intervals studied thus far. It has been proposed that hydrocarbon generation and migration began prior to the deformation event, known as the Baikalian orogeny, that created the

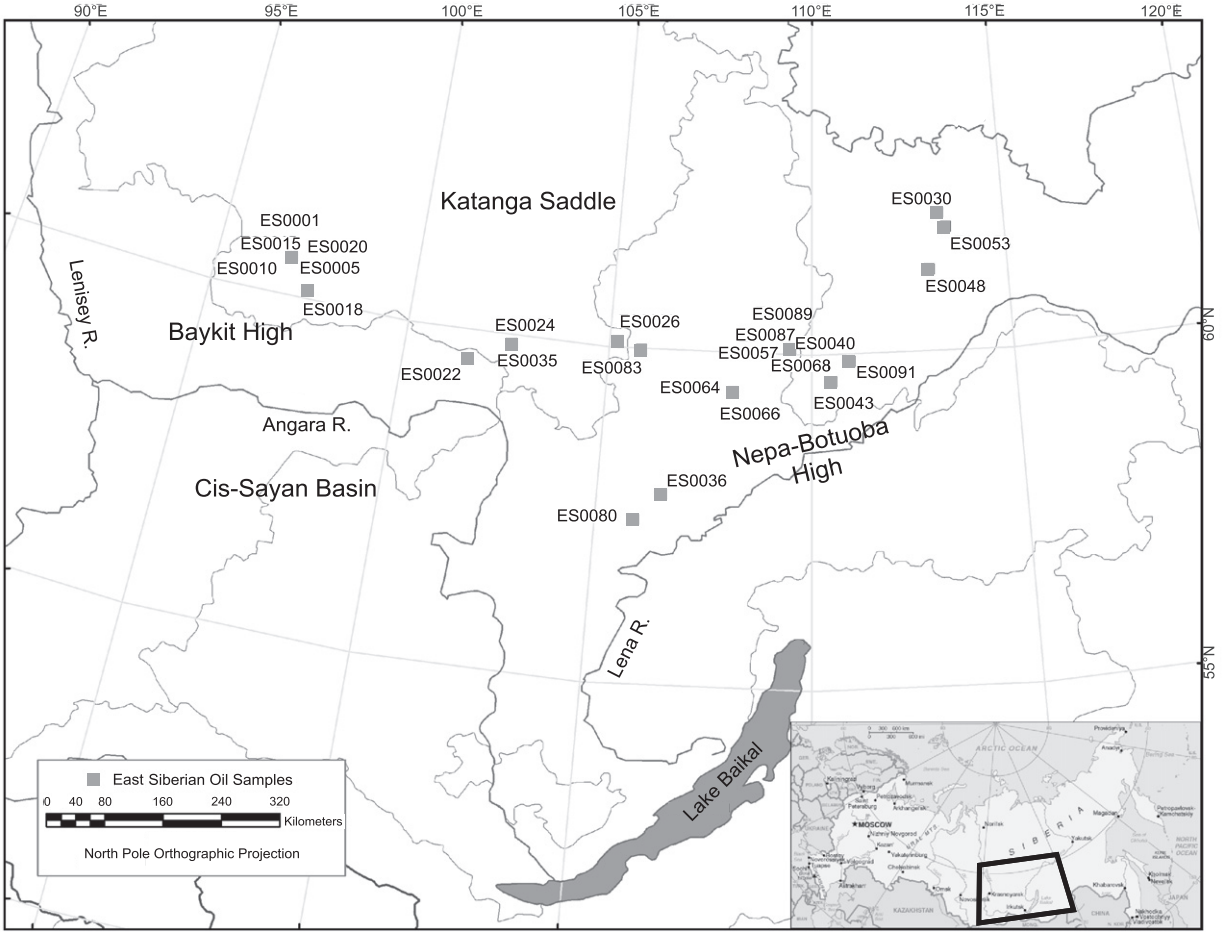

Fig. 1. Map, adapted from Ulmishek (2001a), showing the localities of the Baykit High region, the Katanga Saddle within the Cis-Sayan Basin and Nepa-Botuoba High region where the eastern Siberian oil samples are reservoired. Inset at lower right shows the area with respect to greater Russia, as adapted from http://www.geographicguide.net/europe/maps-europe/maps/russia-europe.gif. (Sokolov and Fedonkin, 1990; Ulmishek, 2001a,b; Mel'nikov et al., 2010) and references therein.

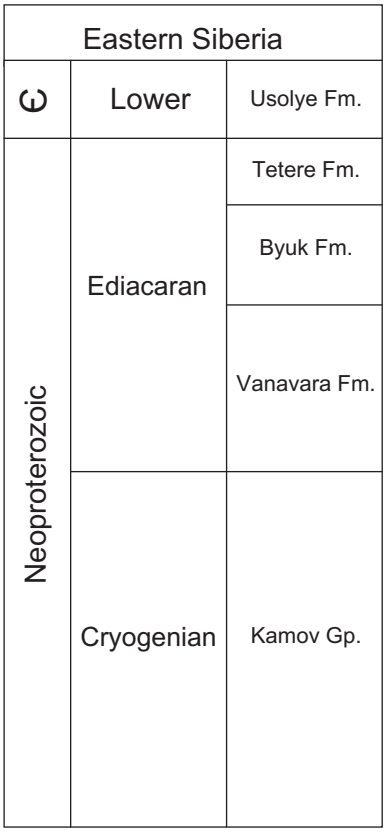

Fig. 2. A chart showing generalized stratigraphic relationships for the habitat and our proposed parent source rock ages of the oils of eastern Siberia based on comparison with geochemical characteristics of Neoproterozoic-Cambrian oils and source rocks from Huqf Supergroup, South Oman Salt Basin (Grosjean et al., 2009). Є denotes Cambrian.

Yenisey Ridge foldbelt and a basin wide pre-Vendian unconformity possibly as early as 850–820 Ma (Ulmishek, 2001a), though there may have been a second (or only) phase of generation during the Paleozoic (Frolov et al., 2011).

The remainder of the oils in this study originated from the contiguous Katanga-Cis-Sayan Basin system and the Nepa-Botuoba High regions of the eastern Siberian Platform (Figs. 1 and 2). All are thought to originate from broadly similar habitats in respect to stratigraphy and petroleum geology. Unlike the habitat of the Baykit High petroleum deposits, the basement is here overlain by Vendian, Cambrian and Ordovician clastic and carbonate sediments and the older Riphean sequences are largely absent. Younger Phanerozoic cover is also thin or absent. Oil and gas are preserved within a narrow stratigraphic interval comprising Vendian and lowermost Cambrian units and sealed beneath undeformed Lower Cambrian salt (Kontorovich et al., 1996; Ulmishek, 2001b). The specific source rocks for the one petroleum system that has been identified are unknown but interpreted to be Riphean and Vendian organic rich shales (Ulmishek, 2001b).

2. Experimental procedures

2.1. Samples

Samples of oils from the eastern Siberian platform were selected from the oil collection of GeoMark Research, Houston, Texas. Pedigree information for the samples is provided in Table 1.

2.2. General procedure

High purity solvents from OmniSolv were used. Prior to use, all glassware and aluminium foil were fired at 550 °C for 8 h and glass wool, pipettes and silica gel were fired at 450 °C for 8 h.

Each sample was fractionated by liquid chromatography on a silica gel 60 (Merck, 230–400 mesh) column using hexane to elute

Table 1
The provenance, age, reservoir lithology and reported depositional environment of the formations in which the eastern Siberian oil samples are currently reservoired. Individual basin names are provided for the Nepa-Botuoba-Katanga oils.

Sample ID	Basin	Formation	Assigned age	Lithology	Depositional environment	Key references
ES0001	Baykit	Kamov group	Riphean	Dolomite with minor sandstone, shale, mudstone and marl	Marine to shallow marine	IHS charts
ES0005						
ES0010						
ES0015						
ES0018						
ES0020						
ES0022	Katanga	Vanavara	Vendian	Shale, dolomite and sandstone	Shallow marine	Ulmishek, 2001b; IHS charts
ES0024						
ES0026						
ES0030	Nepa-Botuoba	Kursov	Vendian	Siltstone and sandstone		Sokolov and Fedonkin, 1990
ES0035	Katanga	Vanavara	Vendian			
ES0036	Nepa-Botuoba	Nepa	Vendian	Siltstone and sandstone	Continental depositional setting	IHS charts
ES0040						
ES0043		Parshino	Vendian			
ES0048		Byuk	Vendian	Dolomite, dolomitic marl and anhydrite		Sokolov and Fedonkin, 1990
ES0053						
ES0057		Katanga	Vendian	Dolomite, clayey dolomite and dolomitic marl	Shallow marine to restricted	Ulmishek, 2001b; IHS charts
ES0064		Tetere	Vendian-Cambrian	Dolomite	Shallow marine to restricted	Ulmishek, 2001b; IHS charts
ES0066						
ES0068						
ES0080		Usol'ye	Lower Cambrian	Salt and dolomite	Shallow marine to restricted	Ulmishek, 2001b; IHS charts
ES0083						
ES0087						
ES0089						
ES0091		Bilir	Lower Cambrian			

the saturated hydrocarbons, 4:1 hexane:dichloromethane to elute the aromatic hydrocarbons and 7:3 dichloromethane:methanol to elute a polar fraction. Activated copper was added to the saturate fraction to remove elemental sulfur. One milligram aliquots of the saturated and aromatic hydrocarbon fractions were added to insert vials with an internal standard and made up to 100 μl with hexane preparatory to gas chromatography–mass spectrometry (GC–MS) analysis. The saturate fractions were analyzed with 50 ng D_4-ααα-24-ethylcholestane (Chiron) as an internal standard while the aromatic fractions were analyzed with 100 ng of D_{14} p-terphenyl (Cambridge Isotope Laboratories).

The saturate fraction was then further separated using 5 Å molecular sieves (1.6 mm pellets from Sigma Aldrich) to trap the *n*-alkanes. The sieves were first activated at 350 °C for 16 h and stored in an airtight jar at 120 °C. The saturated fraction was dissolved in cyclohexane and transferred into a 3 ml Reacti-vial. For every 10–20 mg of saturates, 0.5 g of sieves were added to the Reacti-vial, which was then amended with cyclohexane up to ~2 ml. The vial was heated at 80 °C overnight after which it was cooled and the sieves filtered, washed with several small portions of cyclohexane and air dried. The *n*-alkanes were then recovered from the sieves using HF and by extracting the solution four times with 1 ml pentane. Where there was enough sample, the isoprenoids were further isolated from the branched/cyclic fraction using a thiourea adduction (Rubinstein and Strausz, 1979).

GC–MS was performed using a Micromass Autospec-Ultima instrument equipped with an Agilent 6890 N series gas chromatograph. For analysis of the saturated hydrocarbons, a 60 m J&W Scientific DB-1 fused silica capillary column (0.25 mm i.d., 0.25 μm film thickness) was used with helium as the carrier gas. Injection was performed at 60 °C in splitless mode and, after a delay of 2 min the oven was programmed from 60 °C to 150 °C at 10 °C/min, then to 315 °C at 3 °C/min where it was held isothermal for 24 min. The source was operated in EI-mode at an ionization energy of 70 eV. For full scan analyses the scan rate was 0.80 s/decade over a mass range of 50–600 *m/z* with a total cycle time of 1.06 s. Data were

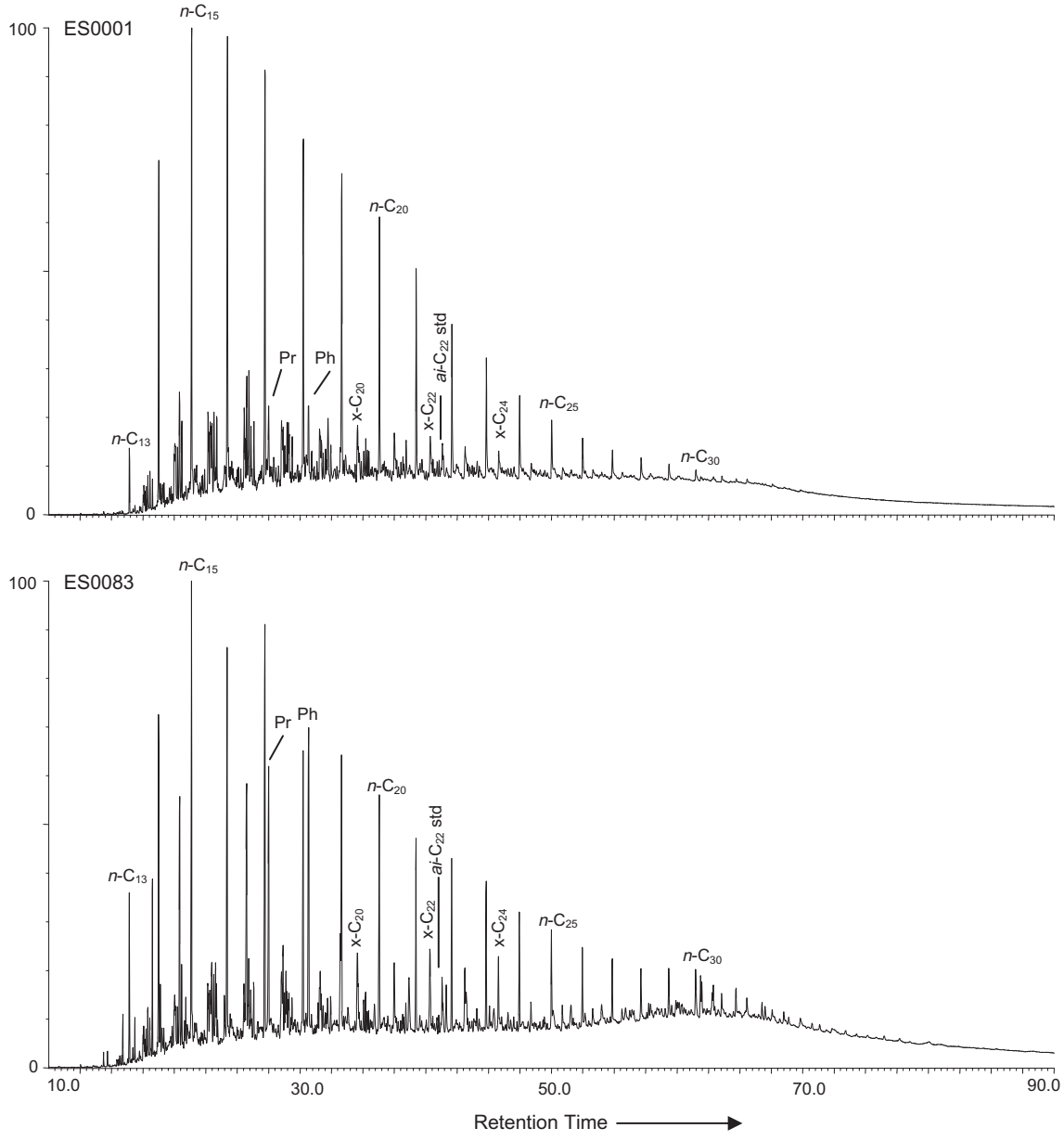

Fig. 3. GC-MS total ion chromatogram showing relative abundances of alkanes, acyclic isoprenoids and mid-chain methylalkanes (X-peaks) in representative oil sample ES0001 (top) of the eastern Siberia Kamov Group from the Baykit High and Vendian-Cambrian oil ES0083 (bottom) from the Usol'ye Formation of the Nepa-Botuoba Basin.

acquired and processed using MassLynx v4.0 software. Alkanes such as *n*-alkanes, pristane, phytane and monomethylalkanes (X-peaks) were quantified using 3-methylheneicosane (*ai*-C_{22}) as internal standard. Biomarkers in the saturated hydrocarbon fraction were analyzed by GC–MS with the Autospec operated in the metastable reaction monitoring (MRM) mode using two time switched groups of precursor-product transitions, the first for cheilanthanes and the second for steranes and triterpanes. The GC was operated under the same conditions as described for the full scan experiments. Peak identification was based on retention time comparisons with the hydrocarbons present in a synthetic standard oil (AGSO Standard Oil) and abundances measured by comparing peak areas to the internal D_4 sterane standard without any adjustment for possible differential responses. Biomarker ratios were obtained using MRM GC–MS analysis.

Aromatics such as aryl isoprenoids were analyzed using a 60 m J&W Scientific DB-5MS GC column (0.25 mm i.d., 0.25 μm film thickness) in selected ion monitoring (SIM) mode. The source and injection methods were the same as for the saturated hydrocarbons. GC–MS analyses of phenanthrene and methylphenanthrenes were performed using an Agilent 7890A GC (splitless injection) interfaced to an Agilent 5975C mass spectrometer. The HP-5 column (50 m × 0.2 mm; 0.11 μm film thickness) was temperature programmed from 150 °C to 325 °C at 2 °C/min (branched/cyclic) and 100 °C to 325 °C at 3 °C/min for aromatics. The mass spectrometer was run in SIM mode, monitoring ions m/z 178 and 192.

Stable carbon isotopic compositions ($^{13}C/^{12}C$) of the bulk C_{15} + saturate and aromatic hydrocarbon fractions were determined using the combustion technique of Sofer (1980) and a Finnigan Delta E isotope ratio mass spectrometer. Results are reported relative to the VPDB standard.

Compound specific carbon isotopic data for *n*-alkanes and acyclic isoprenoids were obtained with a ThermoFinnigan Trace GC equipped with a J&W DB-1MS column (60 m × 32 mm, 0.25 μm film). Chromatographic conditions were initially 60 °C for 3 min, ramped from 60–180 °C at 10 °C/min, then to 320 °C at 4 °C/min, and finally held at 320 °C for 40 min. The GC was coupled to a combustion furnace interfaced to a Finnigan MAT Delta Plus XP isotope ratio monitoring mass spectrometer operated with Isodat 2.0. Precision of isotope results was measured with standards and found to be better than 0.35‰ vs. VPDB and sample replicates produced average errors of ~0.4‰ vs. VPDB.

Principal components analysis and hierarchical cluster analysis were conducted using Pirouette Lite software (Infometrix Corporation).

3. Results

Inspection of the total ion current data from the full scan GC–MS revealed two distinct hydrocarbon distributions in the set of oils. Some of the oils, typified by the Baykit High sample ES0001, shown in the top panel of Fig. 3, have low abundances of pristane (Pr), phytane (Ph) and mid-chain monomethylalkanes (sometimes termed X-peaks) relative to *n*-alkanes. The remainder, typified by the Nepa-Botuoba sample ES0083, shown in the bottom panel of Fig. 3, have much higher relative abundances of acyclic isoprenoids and X-peaks. All of the saturated hydrocarbon fractions have a unimodal distribution of *n*-alkanes, a high content of unresolved components and low Pr/Ph ratios.

The Pr/Ph data are suggestive of source rocks deposited in reducing environments (Table 2). Homohopane indices are typically near 10% with similar values for the gammacerane/hopane ratios. Maturity sensitive biomarker proxies (Table 3) show that the oils are all mature, but not overmature considering their age. Values of Ts/(Ts + Tm) average near 0.55 for the Baykit High oils with C_{31} homohopane and sterane epimer ratios near to their endpoint values 0.6 and 0.55 respectively. Nepa-Botuoba-Katanga oils appear, on average, to be slightly less mature with values of Ts/(Ts + Tm) near 0.45 and moretane/hopane ratios lower than for the Baykit High samples. This is consistent with their higher values for Ph/*n*-C_{18} and methylphenanthrene index (MPI1).

Table 2
Biomarker redox and stratification proxies showing differences in the depositional environment of the Baykit High samples (ES0001–ES0020) compared to the Nepa-Botuoba-Katanga type samples (ES0022–ES0091). The homohopane index was calculated as $C_{35}H$ (R + S) * 100/C_{31}–$C_{35}H$ (R + S)%. The isomers referred to in the ratios C/(A + B) and C/A are C_{19} norsteranes.

	Pr/Ph	Homohopane index %	Gamm./$C_{30}H$	Steranes 21-norC_{28}/C28αββR	Steranes 21-norC_{28}/C_{28}	C/(A + B)	C/A
Biomarker proxies for water column redox and/or stratification							
ES0001	0.94	8.01	0.09	0.39	0.08	0.11	0.71
ES0005	1.06	9.57	0.09	0.38	0.08	0.09	0.60
ES0010	0.89	8.98	0.10	0.23	0.05	0.12	0.77
ES0015	1.26	9.59	0.10	0.43	0.10	0.10	0.59
ES0018	1.01	9.13	0.11	0.33	0.08	0.13	0.80
ES0020	1.14	8.46	0.07	0.25	0.05	0.12	0.85
ES0022	0.75	9.93	0.11	0.45	0.11	0.14	0.74
ES0024	0.79	9.91	0.10	0.29	0.07	0.15	0.77
ES0026	0.77	7.48	0.08	0.23	0.06	0.13	0.75
ES0030	0.83	10.85	0.13	0.30	0.07	0.15	0.75
ES0035	0.76	8.98	0.08	0.24	0.06	0.12	0.91
ES0036	0.72	8.66	0.09	0.50	0.10	0.10	0.58
ES0040	0.68	10.43	0.07	0.31	0.08	0.19	1.06
ES0043	0.77	9.47	0.09	0.33	0.09	0.11	0.67
ES0048	0.66	11.90	0.07	0.21	0.05	0.09	0.55
ES0053	0.85	12.25	0.08	0.32	0.07	0.08	0.48
ES0057	0.74	8.21	0.07	0.23	0.06	0.20	1.45
ES0064	0.69	9.71	0.07	0.21	0.06	0.18	0.98
ES0066	0.67	8.55	0.09	0.37	0.10	0.11	0.72
ES0068	0.72	11.12	0.07	0.23	0.06	0.13	0.98
ES0080	0.74	5.80	0.11	0.35	0.09	0.07	0.45
ES0083	0.75	9.69	0.07	0.22	0.05	0.12	0.82
ES0087	0.63	9.82	0.07	0.24	0.06	0.21	1.38
ES0089	0.64	9.93	0.08	0.31	0.08	0.12	0.77
ES0091	0.76	10.06	0.07	0.34	0.08	0.12	0.78

Steranes are abundant in all of the samples. Sterane/hopane ratios average near to 0.65 in Baykit High samples as compared to the Nepa-Botuoba-Katanga oils with values always >1 and as high as 4.6 (Table 4). Without exception, C_{29} steranes dominate over C_{27} and there is a significant complement of C_{30} steranes comprising both 24-*n*-propylcholestanes and 24-isopropylcholestanes (Ta-

Table 3
Biomarker maturity proxies suggesting that all of the oils are of moderate thermal maturity, with the Baykit High samples being slightly more mature, and ES0080 having an anomalous abundance of Ts. The odd/even predominance (OEP) index is measured as (n-C_{25} + 6 * n-C_{27} + n-C_{29})/(4 * n-C_{26} + 4 * n-C_{28}). A new parameter for low molecular weight (LMW) OEP is defined as (n-C_{17} + n-C_{19})/(n-C_{16} + n-C_{18}). Methyl phenanthrene index 1 (MPI1) is defined as [1.5(2-MeP + 3Me-P)/(P + 1-MeP + 9-MeP)], where P denotes phenanthrene. NM = not measured.

	Ts/(Ts + Tm)	C_{31} hopanes 22S/(S + R)	C_{29} steranes ααα 20S/(S + R)	C_{30} hopanes βα/(αβ + βα)	Ts/hopane	Ph/n-C_{18}	OEP	LMW OEP	MPI1
Biomarker proxies for maturity									
ES0001	0.52	0.66	0.54	0.05	0.38	0.24	0.98	0.93	0.79
ES0005	0.58	0.59	0.51	0.05	0.38	0.20	0.99	0.94	0.89
ES0010	0.51	0.59	0.54	0.05	0.41	0.22	0.96	1.02	0.89
ES0015	0.63	0.59	0.54	0.05	0.51	0.14	0.96	0.93	0.97
ES0018	0.63	0.65	0.58	0.05	0.49	0.18	0.99	0.95	0.94
ES0020	0.52	0.51	0.51	0.08	0.36	0.19	0.97	0.94	0.89
ES0022	0.58	0.52	0.55	0.08	0.48	0.51	0.99	1.06	0.40
ES0024	0.43	0.52	0.54	0.07	0.32	0.86	0.99	1.00	0.47
ES0026	0.43	0.52	0.54	0.07	0.35	1.11	0.97	1.22	0.35
ES0030	0.38	0.58	0.52	0.07	0.32	1.08	0.98	1.08	0.62
ES0035	0.42	0.51	0.53	0.06	0.23	0.95	0.93	1.02	0.46
ES0036	0.67	0.57	0.54	0.06	0.64	0.95	1.05	1.39	NM
ES0040	0.41	0.52	0.52	0.06	0.31	1.38	0.95	1.12	0.68
ES0043	0.37	0.58	0.53	0.06	0.34	1.22	0.96	1.13	0.70
ES0048	0.38	0.60	0.54	0.05	0.25	1.38	1.00	1.24	0.56
ES0053	0.45	0.60	0.55	0.04	0.23	1.05	0.98	1.06	0.53
ES0057	0.40	0.59	0.52	0.05	0.29	1.43	1.00	1.06	0.66
ES0064	0.57	0.56	0.51	0.05	0.50	1.56	1.02	1.02	NM
ES0066	0.56	0.59	0.56	0.05	0.67	1.24	1.02	1.06	NM
ES0068	0.40	0.59	0.54	0.05	0.29	1.35	1.03	1.13	0.68
ES0080	0.72	0.53	0.57	0.04	1.11	1.23	0.94	1.06	NM
ES0083	0.37	0.57	0.53	0.05	0.26	1.39	0.99	1.06	0.63
ES0087	0.43	0.59	0.52	0.05	0.31	1.64	1.04	1.08	0.64
ES0089	0.48	0.54	0.57	0.05	0.34	1.38	1.00	1.42	NM
ES0091	0.39	0.58	0.52	0.05	0.28	1.31	0.93	1.10	0.68

Table 4
A selection of biomarker ratios widely considered to be diagnostic for source organisms and showing some marked differences in the biotic inputs to the Baykit High samples (ES0001–ES0020) compared to the remainder (ES0022–ES0091). The 2- and 3-methylhopane indices, calculated as X-Mehopane/(X-Mehopane + hopane) * 100, suggest input from both cyanobacteria and methanotrophic proteobacteria, respectively. C_{27}/C_{29} steranes ratios ~0.2 suggest a predominance of organic matter from green algae in all of these samples. In particular, algal steroids predominate of bacteriohopanes and there is a significantly higher abundance of mid-chain methylalkanes in the Nepa-Botuoba-Katanga type oils. 24-isopropylcholestanes and 24-*n*-propylcholestanes are abbreviated as *i*-C_{30} and *n*-C_{30}.

	Steranes/ hopanes	2α−MeHI %	3β−MeHI %	Hopanes 28,30-dinor/ C30αβ	Steranes C_{27}/C_{29}	n-C_{22}/x-C_{22}	n-C_{24}/x-C_{24}	x-C_{20}/ Ph	Steranes i-C_{30}/ n-C_{30}	Steranes i-C_{30} αααR/n-C_{30} αααR
Biomarker proxies for source organisms										
ES0001	0.61	6.55	3.59	0.18	0.20	2.66	2.68	0.90	3.03	1.81
ES0005	0.67	8.30	4.64	0.17	0.16	3.33	2.79	1.10	2.52	2.20
ES0010	0.63	8.78	5.50	0.18	0.17	3.08	3.10	0.96	2.73	1.70
ES0015	0.72	8.47	5.58	0.17	0.21	3.71	2.66	1.31	1.73	0.96
ES0018	0.73	6.10	4.33	0.18	0.19	3.89	3.35	0.95	2.37	1.15
ES0020	0.85	8.44	5.22	0.17	0.33	2.99	3.17	0.96	0.74	0.32
ES0022	0.47	12.69	8.60	0.14	0.15	2.44	2.40	0.44	1.75	1.91
ES0024	0.64	11.01	5.39	0.24	0.17	1.47	1.25	0.42	2.78	1.20
ES0026	0.86	11.09	5.57	0.42	0.16	1.26	1.14	0.40	2.28	1.21
ES0030	0.86	10.47	6.34	0.32	0.17	1.96	2.59	0.32	2.95	1.76
ES0035	0.61	9.13	4.30	0.13	0.15	1.51	1.32	0.49	2.76	1.27
ES0036	2.23	8.42	5.46	0.42	0.18	1.20	1.18	0.53	1.12	0.52
ES0040	1.26	10.73	4.77	0.39	0.18	1.31	1.25	0.25	2.43	1.38
ES0043	1.20	11.31	4.95	0.37	0.16	1.28	1.19	0.37	2.09	1.75
ES0048	0.82	6.67	4.22	0.15	0.20	1.34	0.79	0.35	2.32	1.77
ES0053	0.79	8.25	4.27	0.12	0.19	1.71	1.63	0.30	2.26	1.63
ES0057	1.10	8.33	3.83	0.30	0.18	1.23	1.22	0.30	2.81	1.24
ES0064	1.77	8.77	3.48	0.55	0.20	1.35	1.21	0.28	1.95	0.99
ES0066	2.59	10.39	4.61	0.52	0.24	1.45	1.54	0.29	1.91	1.36
ES0068	1.01	8.61	3.94	0.30	0.19	1.30	1.25	0.31	2.10	1.24
ES0080	4.63	8.74	5.43	0.41	0.30	1.36	1.92	0.26	1.43	0.51
ES0083	1.00	8.54	3.78	0.25	0.22	1.36	1.53	0.23	2.22	1.03
ES0087	1.10	8.36	3.89	0.30	0.19	1.16	1.15	0.29	1.97	1.09
ES0089	1.34	10.15	4.89	0.28	0.18	1.38	1.28	0.35	2.20	1.32
ES0091	1.03	9.39	4.04	0.34	0.17	1.25	1.05	0.41	2.01	1.41

ble 4). Triterpanes that are prominent in all samples include 28,30-dinorhopane and homologous series of 2- and 3-methylhopanes (Table 4).

The aromatic hydrocarbon fraction showed that aryl isoprenoids were not detected in the 133 or 134 *m/z* ion chromatograms. However, the Baykit High samples were distinguished from the Nepa-Botuoba-Katanga oils on the basis of the methylphenanthrene index MPI1, which is defined as [1.5(2-MeP + 3Me-P)/(P + 1-MeP + 9-MeP)], where P denotes phenanthrene. The Baykit High samples are slightly more mature with values that range from 0.79–0.97 (average = 0.9) whereas the Nepa-Botuoba-Katanga oils have lower indices with a range in values from 0.35–0.70 (average = 0.58) (Table 3).

Isotopic values of saturated hydrocarbon fractions in the Baykit High oils cluster tightly near to −33.5‰, while the Nepa-Botuoba-Katanga oil values are generally 1–2‰ more negative. Compound specific carbon isotope analyses provide a further distinctive difference between the Baykit High oils whose acyclic isoprenoids (Pr and Ph) are more depleted than their *n*-alkane counterparts, whereas the opposite relationship exists for the Nepa-Botuoba-Katanga oils.

4. Discussion

4.1. Acyclic hydrocarbons

The low Pr/Ph ratios for all the samples in the study suggests they originated from sediments deposited under anoxic conditions and, likely, under stratified water columns (Powell and McKirdy, 1973; Didyk et al., 1978; ten Haven et al., 1987). Empirical evidence suggests that a Pr/Ph value < 0.8 is diagnostic for an anoxic environment as commonly encountered in strongly stratified water columns. Ratios of Pr/Ph > 1 suggests slightly more oxygenated environments, while Pr/Ph > 3 is generally observed in settings where terrigenous organic matter is transported and deposited in oxygenated water (Peters et al., 2005). As shown in Table 2 and Fig. 3, the Pr/Ph values are around 1 for the Baykit High oils and significantly lower, between 0.6 and 0.85, for the remainder of the samples. This suggests that the oils of the Baykit High may be derived from marine source rocks that were deposited in slightly more oxidizing or less restricted conditions than those that generated the Nepa-Botuoba-Katanga oils.

The phytane/*n*-C_{18} ratio can serve as a maturity proxy (ten Haven et al., 1987). Values ≫1 suggest a sample is immature. This ratio is also often used as an indicator for biodegradation. Within any family of oils, slightly to moderately biodegraded oils have higher phytane/*n*-C_{18} ratios (Peters et al., 2005). The Baykit High oils have values around 0.2, whereas most of the other samples have values >1. Samples ES0022 and ES0024 fall in between. Superficially, this suggests that the Baykit High samples are slightly more mature than the Nepa-Botuoba-Katanga oils. On the other hand, the low relative abundances of acyclic isoprenoids and X-peaks, overall, are more readily understood as reflecting a significant difference in organic source facies between the Nepa-Botuoba-Katanga and Baykit High oil types.

Homologous series of X-peaks are a prominent constituent of Proterozoic oils and sedimentary rocks across multiple continents (Klomp, 1986; Fowler and Douglas, 1987; Summons and Powell, 1992; Höld et al., 1999; Logan et al., 1999; Luo et al., 2008). The source of these compounds is not known although cyanobacteria, sponges and colorless sulfide oxidizing bacteria (Shiea et al., 1990; Thiel et al., 1999; Love et al., 2008) have been postulated as precursor organisms. A visual comparison of Figs. 3 and 4a and two ratios provided in Table 4, *n*-C_{22}/*x*-C_{22} and *n*-C_{24}/*x*-C_{24}, identify the Nepa-Botuoba-Katanga oils as having a relatively higher content of X-peaks than the Baykit High oils and, in this respect together with their relatively high contents of acyclic isoprenoids (i.e. low *x*-C_{20}/Ph), they are not distinguishable from the Huqf oils from Oman (Klomp, 1986; Grosjean et al., 2009). Furthermore, a slight even/odd predominance of these mid-chain methylalkanes, especially in the C_{18}–C_{24} range (Fig. 3), is seen for the Nepa-Botu-

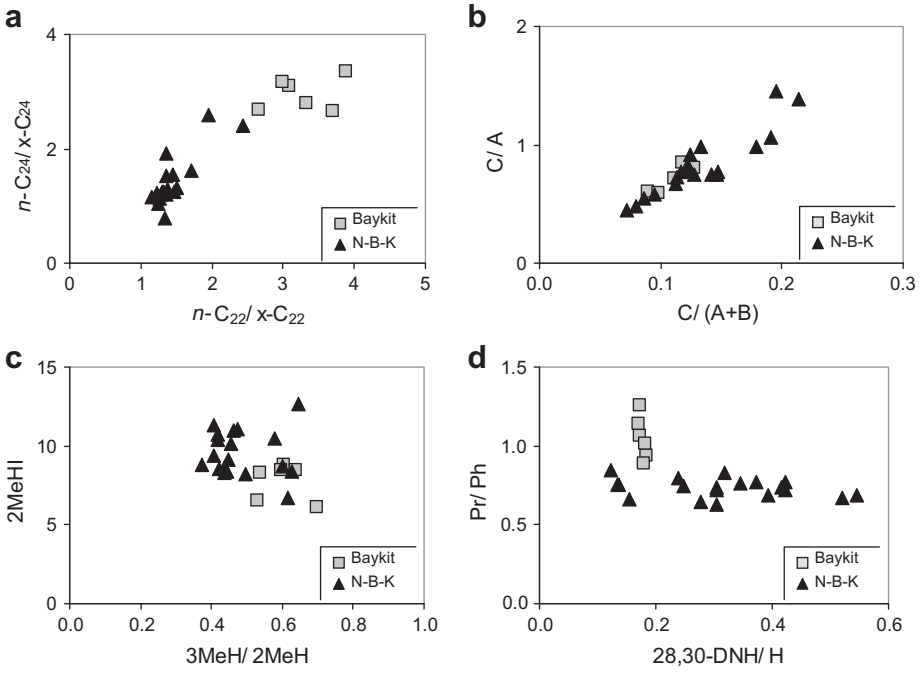

Fig. 4. Cross plots for a selection of biomarkers to illustrate the geochemical differences between Riphean and Vendian-Cambrian oil families of the eastern Siberian Platform. Samples from the Baykit High are denoted by grey squares, whereas the Nepa-Botuoba-Katanga (N-B-K) oils are denoted by black triangles. (a) *n*-C_{24}/x-C_{24} vs. *n*-C_{22}/x-C_{22}; (b) C_{19} norsteranes C/A vs. C/(A + B); (c) 2-methylhopane index (2-methylhopane/(2-methylhopane + hopane)) vs. 3-methylhopane/2-methylhopane; (d) pristane/phytane vs. 28,30-dinorhopane/hopane.

oba-Katanga oils but not for the Baykit High oils suggesting a lower thermal maturity for the former. The alkane odd/even predominance (OEP) is defined here as (n-C_{25} + 6 ∗ n-C_{27} + n-C_{29})/(4 ∗ n-C_{26} + 4 ∗ n-C_{28}). All of the oils in the study set have OEPs around 1 consistent with them being thermally mature and devoid of land plant derived hydrocarbons (Scalan and Smith, 1970). Low molecular weight alkanes, in contrast, show a distinct odd carbon number preference, but only in the Baykit High samples. A new parameter for low molecular weight (LMW) OEP, defined as (n-C_{17} + n-C_{19})/(n-C_{16} + n-C_{18}), shows this feature (Table 3). The patterns observed (Fig. 3) are quite unusual for rocks of this apparent age and reminiscent of oils and sediments of Cambro-Ordovician

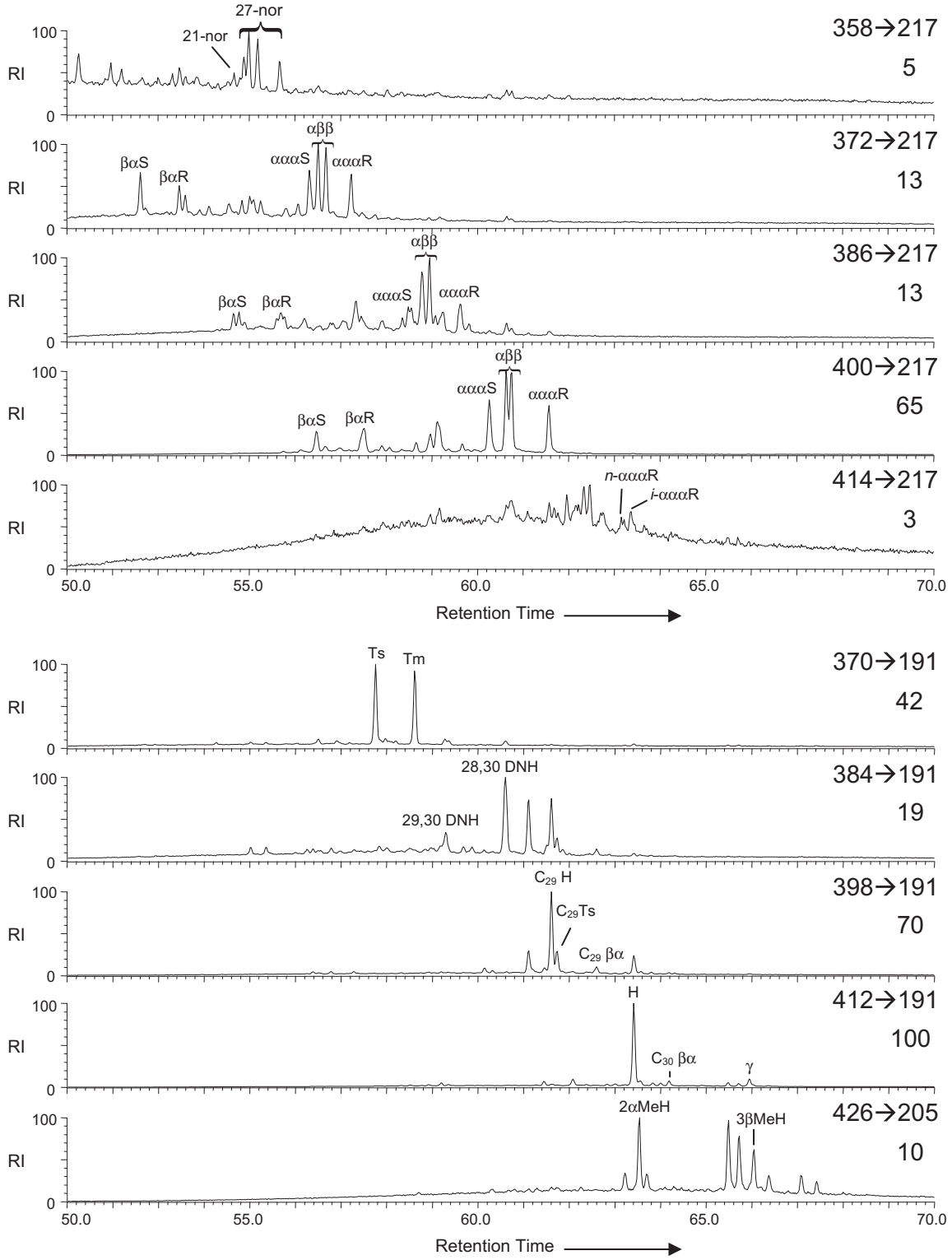

Fig. 5. A selection of GC-MS MRM chromatograms showing relative abundances of steranes (top) and hopanes (bottom) in a representative oil sample (ES0001) from the Baykit High, with transitions and relative intensities. The isomers are labeled where diasteranes are designated as βαS or βαR and steranes are αααS, αββ (where the brackets include R and S), and αααR. Ts is 18α(H)-trisnorneohopane, Tm is 17α(H)-trisnorhopane, DNH is 28,30-dinorhopane, C_{29}Ts is 18α-30-norneohopane, H is hopane and γ is gammacerane.

age with contributions of organic matter from *G. prisca* (Foster et al., 1989).

4.2. Triterpenoids and steroids

Representative distributions of steroids and triterpenoids for Baykit High and Nepa-Botuoba-Katanga oils are shown in Figs. 5 and 6 respectively. Ts/(Ts + Tm) values are commonly used to evaluate thermal maturity, with higher values indicating higher maturities (Seifert and Moldowan, 1978). However, there is a strong sedimentary facies control on this ratio, so it is most reliable when compared among oils of similar sources. The Ts/(Ts + Tm) ratios vary from around 0.4–0.7 (Table 3). The αβ-homohopane 22S/(22S + 22R) and C_{29} ααα sterane 20S/(20S + 20R) ratios can also

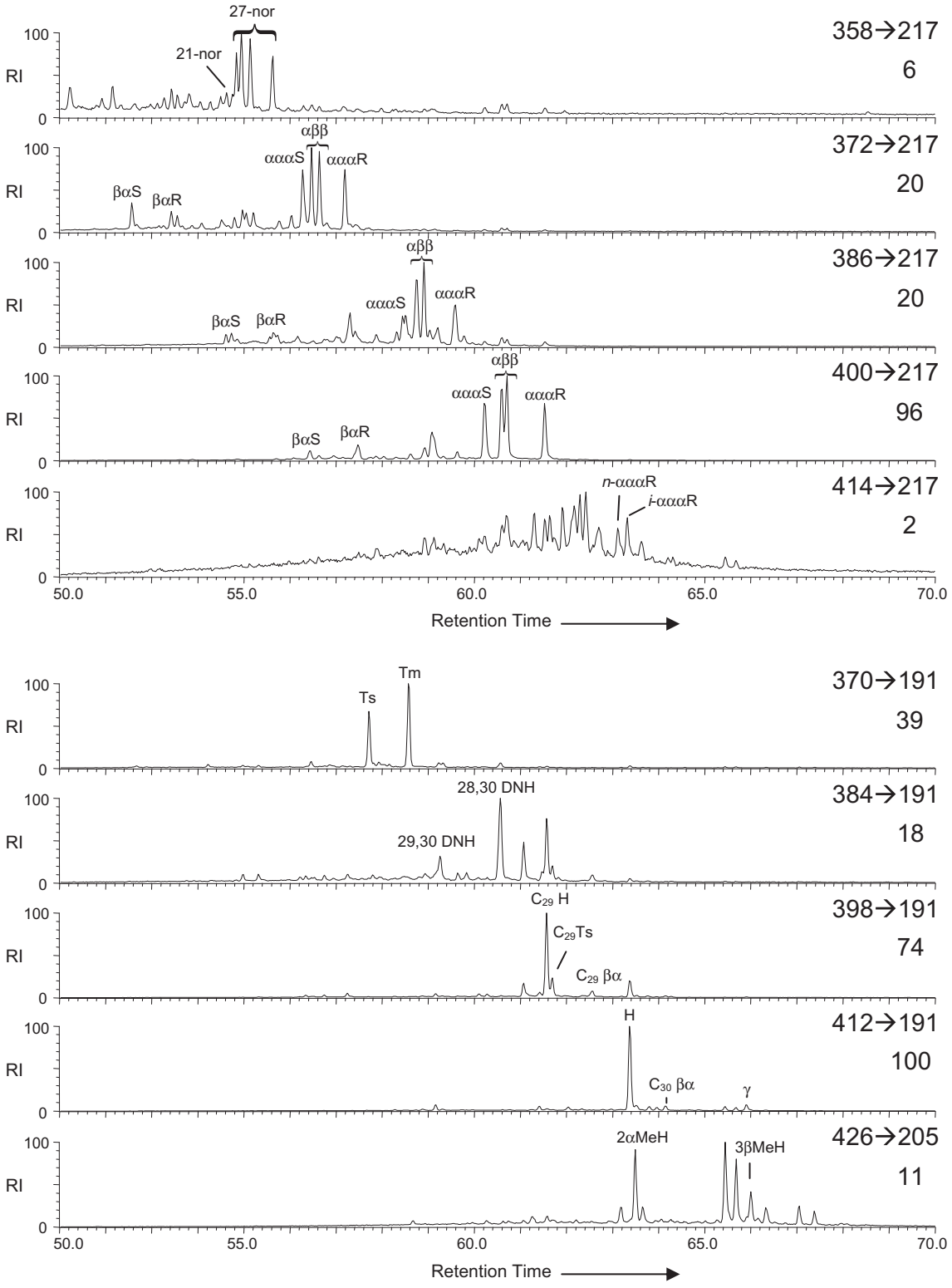

Fig. 6. A selection of GC-MS MRM chromatograms showing relative abundances of steranes (top) and hopanes (bottom) in a Vendian-Cambrian oil (ES0083) from the Usol'ye Formation from the Nepa-Botuoba Basin, with transitions and relative intensities. Compound abbreviations as in Fig. 5.

be used to assess thermal maturity. Values at or near 0.55 indicate mature samples, as do high C_{30} hopane/moretane ratios (Seifert and Moldowan, 1980). The homohopane 22S/(22S + 22R) ratios are all >0.55 and the sterane 20S/(20S + 20R) values are all between 0.5 and 0.6, consistent with moderate levels of thermal maturity across the oil set. The moretane/(moretane + hopane) ratios are all around 0.05 (Peters et al., 2005), with the exception of samples ES0020–ES0043, which are between 0.07 and 0.08 and thus are slightly less mature. For post-mature samples, Ts/hopane can be used as a maturity proxy (Volkman et al., 1983). The samples all have values between 0.2 and 0.7, except for sample ES0080 which also has the highest Ts/(Ts + Tm) value.

Two proxies widely used to assess water column stratification (see Table 2) are the C_{35} homohopane index, measured as C_{35}H (R + S) $*$ 100/C_{31}–C_{35}H (R + S)% and the gammacerane/hopane ratio (Peters et al., 2005). Gammacerane is formed through the dehydration-reduction and/or sulfurization of tetrahymanol (ten Haven et al., 1989; Harvey and McManus, 1991; Sinninghe Damsté et al., 1995), a sterol surrogate produced by bacteriovorous ciliates that feed at the density interfaces of stratified water columns (ten Haven et al., 1989; Harvey and McManus, 1991). The values for the homohopane index are all around 10% and the gammacerane/hopane ratios are all around 0.1 which would be consistent with source rock deposition at normal marine salinities as opposed to highly stratified or hypersaline conditions. Data on oils from the roughly coeval South Oman Salt Basin (SOSB) suggest that the abundance of 21-norsteranes (relative to C_{28} steranes) and an unidentified C_{19} norsterane (tentatively identified as a steroid with a carbon missing from the A or B ring) that has been referred to as compound C (Grosjean et al., 2009) relative to other C_{19} norsteranes simply named as A and B may also be potential indicators of water column stratification, since they, along with the gammacerane to hopane ratio and the homohopane index, increase markedly within the Ara evaporite sequence compared to the underlying Nafun Group rocks (Grosjean et al., 2009). In the eastern Siberia oil set, all these salinity/stratification proxies are, on average, significantly lower than those of the Ara Group source rocks and oils of Oman. This suggests that the source rocks for the Siberian oils were deposited in less restricted paleoenvironments. The cross plot of C/A vs. C/(A + B), where A, B, and C are the C_{19} norsterane isomers, shows a linear correlation where the Baykit High samples group more tightly than the Nepa-Botuoba-Katanga oils (Fig. 4b).

The 2-methylhopane index (2MeHI) has been proposed as a molecular proxy for cyanobacteria (Summons et al., 1999). Although these biomarkers are also known from the Rhizobiales group of the alphaproteobacteria (Rashby et al., 2007; Welander et al., 2010), a specific physiological role has been identified in heterocystous cyanobacteria (Doughty et al., 2009) and a cyanobacterial source for these compounds is generally more consistent with the marine sedimentary environments indicated by other proxies. Further, Rhizobiales bacteria are one potential source of tetrahymanol, the biological precursor of gammacerane. The low relative abundance of gammacerane (gammacerane/hopane ~0.07–0.13) in the eastern Siberia oils stands in contrast to its, overall, higher relative abundance in SOSB oils (gammacerane/hopane ~0.1–0.3) suggesting that the sources of gammacerane and 2-methylhopanes are distinct. The 2MeHI values are all between 6% and 12% which is a similar range of values to those seen in Phanerozoic shales and marls and in oils and their source rocks from the SOSB (Grosjean et al., 2009). The 3-methylhopane index (3MeHI) is potentially useful as a proxy for methanotrophic proteobacteria (Collister et al., 1992; Farrimond et al., 2004) and the 3MeHI values are all between 3% and 9%, significantly higher than the typical Phanerozoic range from 1% to 3%, suggesting a modest but significant input from Type I methanotrophic proteobacteria (Fig. 4c) and an active methane cycle during deposition of both the Baykit High and Nepa-Botuoba-Katanga source rocks.

The 28,30-dinorhopane to C_{30} hopane ratio, when high, suggests a clay poor, anoxic depositional environment (Peters et al., 2005) meaning oxic surface waters but with anoxic/sulfidic porewaters or bottom waters and a compressed redox gradient. The Baykit High oil values are all around 0.18, whereas the Nepa-Botuoba-Katanga oils values range between 0.12 and 0.55, with an average of 0.3 (Fig. 4d). Superficially, this suggests a more oxygen deprived sedimentary environment for the latter oils. However, given the higher abundances of diasteranes relative to steranes in the Baykit High oils, and their elevated thermal maturity, it is difficult to tease apart these confounding controls on 28,30-dinorhopane abundances.

The ratio of steranes to hopanes is primarily used as an indicator of input from eukaryotes (mainly algae) relative to bacteria (Moldowan et al., 1985). The values for Baykit High samples are all <0.9 whereas those from the Nepa-Botuoba-Katanga system oils have, on average, ratios >1. The difference is probably significant and represents a higher algal contribution to the Nepa-Botuoba-Katanga oils. In all cases, the C_{29} steranes dominate the distributions with C_{27}/C_{29} sterane ratios averaging ~0.2. These data suggest that algae from the green line of descent (i.e. Chlorophyceae), and possibly including basal lineages of the Prasinophyceae, were ecologically important in the sedimentary environments of both basins (Kodner et al., 2008). Conversely, with the C_{28}/C_{27} ratios of 1 or less in combination with C_{28}/C_{29} ratios of <0.25, these data also suggest that the chlorophyll c algae were ecologically unimportant contributors to the sedimentary organic matter sourcing these oils (Knoll et al., 2007).

One steroid proxy that is elevated during this time period is the ratio of 24-isopropylcholestanes to 24-*n*-propylcholestanes, now established as a robust biomarker for demosponges (McCaffrey et al., 1994; Love et al., 2009). It may also serve as an age proxy since it is only found to be high ($\geqslant$0.5) in Neoproterozoic to Ordovician age rocks and oils (McCaffrey et al., 1994; Love et al., 2009) and the earliest detection of 24-isopropylcholestanes is between the Sturtian and the Marinoan glaciation events between 713–635 Ma (Love et al., 2009). The distributions of sterols in extant organisms suggest that *n*-propyl isomers of the C_{30} desmethylsteranes likely originate from a marine algal source (Pelagophyceae) while the sterol precursors of the isopropyl isomers are only found in significant amounts in demosponges (Love et al., 2009). Molecular clock studies indicate that demosponges, being the most basal metazoan clade, diverged from the last common ancestor of all metazoans in the Neoproterozoic (Peterson et al., 2004, 2005), prior to the first sedimentary record of spicules or other established sponge fossils. A rationalization of molecular phylogenies, paleontological and geochemical data suggests that sponges may have experienced a period of ecological prominence during the Neoproterozoic to early Paleozoic, allowing for a rise in the 24-isopropylcholestanes to 24-*n*-propylcholestanes ratio. Because they consume dissolved and particulate organic matter, it has been further hypothesized that they may have been an important factor in the Ediacaran reorganization of biogeochemical cycles and protracted oceanic ventilation, and declined thereafter (Sperling et al., 2007). Almost all of the eastern Siberia oil samples (exceptions are ES0020, ES0036 and ES0080) have 24-isopropylcholestanes/24-*n*-propylcholestanes ratios well in excess of unity suggesting that demosponges were a significant component of the biota in the ancient sedimentary environments that sourced these hydrocarbons. In this respect, the eastern Siberian oils closely resemble their Neoproterozoic counterparts from the SOSB (Grosjean et al., 2009; Love et al., 2009). Speculatively, the Baykit High sample (ES0020), with a much lower 24-isopropylcholestanes/24-*n*-propylcholestanes ratio, may be an end member from a

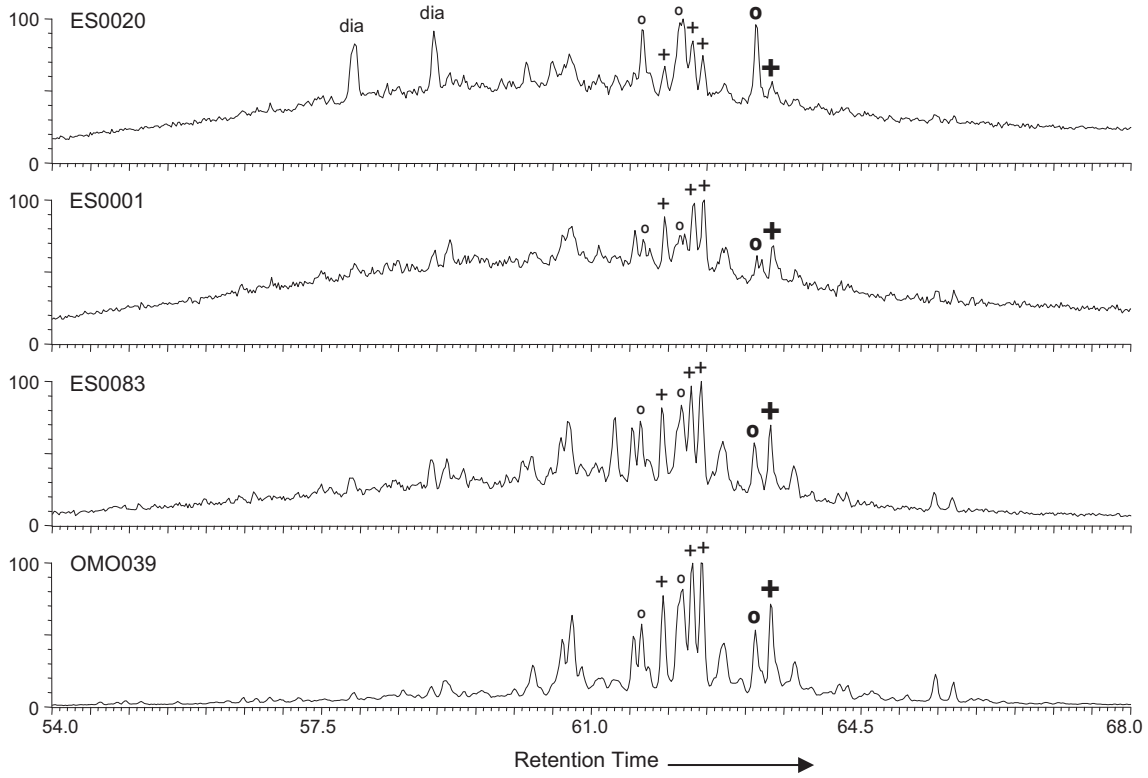

Fig. 7. GC-MS MRM chromatograms for 414→217 transition for potentially the oldest end member (ES0020), a Baykit High oil (ES0001), a Nepa-Botuoba-Katanga oil (ES0083) and a carbonate stringer oil from A3C (OMO039) to demonstrate the presence of 24-isopropylcholestane isomers in most of the eastern Siberian oils. All four regular diastereoisomers [ααα*S*, αββ (R + S), ααα*R*) of 24-isopropylcholestane (+) and 24-*n*-propylcholestane (o) are designated, with the larger, bold symbols indicating the ααα*R* isomers as labeled in Figs. 5 and 6.

pre-Cryogenian source rock. A comparison of this potential end member (ES0020), a Baykit High sample (ES0001), a Nepa-Botuoba-Katanga oil (ES0083) and an A3C carbonate stringer oil from the SOSB (OMO039) that was previously demonstrated to have a high 24-isopropylcholestanes/24-*n*-propylcholestanes ratio (Grosjean et al., 2009) is presented in Fig. 7 and demonstrates the comparative lack of 24-isopropylcholestane isomers in ES0020 compared to the other eastern Siberian oils, which are more similar to the SOSB oil.

4.3. Carbon isotopic data

The isotopic compositions of bulk saturated and aromatic hydrocarbons (Table 5) show the ^{13}C depleted signatures that are typical of Neoproterozoic-Cambrian petroleum samples and which distinguish them from Phanerozoic oils and bitumens (Sofer, 1984; Fowler and Douglas, 1987; Grantham et al., 1988; Andrusevich et al., 1998; Grosjean et al., 2009). Further, the samples appear to fall into two broad groups. Isotopic values of saturated hydrocarbon fractions in one group cluster tightly near to −33.5‰, while in another group values are generally 1–2‰ more negative. The former group comprises all of the Baykit High oils.

Carbon isotopic compositions of *n*-alkanes and acyclic isoprenoids were also measured in all the samples and results for these hydrocarbons are presented in Table 5. The oils of the Baykit High and Katanga Saddle contain acyclic isoprenoids (Pr and Ph) that are more depleted than their *n*-alkane counterparts, whereas the opposite relationship exists for the Nepa-Botuoba oils. The value Δ is calculated as the difference between the average carbon isotopic composition of *n*-alkanes (n-C_{17} and n-C_{18}) minus the average

Table 5
A summary of $\delta^{13}C$ values for bulk saturated and aromatic hydrocarbons as well as data for individual alkanes in eastern Siberian oils. The values for C_{17} and C_{18} *n*-alkanes and the isoprenoids pristane and phytane show an inverted pattern, where *n*-alkanes are isotopically enriched in ^{13}C compared to isoprenoids leading to a positive difference between them (Δ), for the Baykit High and Katanga Saddle samples as compared to those from the Nepa-Botuoba group. Where there is no value, the peaks were too small to be measured reliably.

	Saturates	Aromatics	n-C_{17}	Pristane	n-C_{18}	Phytane	Δ
Bulk and compound specific carbon stable isotope signatures							
ES0001	−33.5	−33.2			−32.5		
ES0005	−33.3	−33.1	−33.2	−35.9	−32.9	−35.3	2.5
ES0010	−33.4	−33.2	−33.3	−43.1	−33.0	−38.8	7.8
ES0015	−−33.4	−33.2	−33.4	−44.6	−33.1	−36.4	7.2
ES0018	−33.4	−33.0	−33.0	−38.2	−32.8	−38.3	5.3
ES0020	−33.3	−32.8	−33.1	−34.6	−32.9	−35.9	2.2
ES0022	−33.9	−33.9	−35.0	−40.3	−34.6	−36.6	3.7
ES0024	−34.4	−34.1	−37.8	−38.7	−36.5	−38.2	1.3
ES0026	−34.5	−34.5	−37.7	−38.2	−36.7	−37.8	0.8
ES0030	−33.9	−35.0	−38.3	−36.3	−36.4	−37.7	−0.4
ES0035	−34.4	−34.1	−37.4	−38.7	−36.2	−39.1	2.1
ES0036	−34.0	−33.2	−36.6	−35.5	−35.4	−34.2	−1.2
ES0040	−35.1	−34.6	−39.0	−37.4	−37.1	−37.5	−0.5
ES0043	−35.1	−34.7	−38.3	−36.3	−36.9	−37.0	−0.9
ES0048	−36.1	−36.5	−38.7	−37.7	−37.7	−38.1	−0.3
ES0053	−35.6	−35.9	−38.2	−36.8	−36.8	−37.4	−0.4
ES0057	−35.1	−34.7	−38.8	−36.7	−37.2	−36.9	−1.2
ES0064	−35.3	−34.6	−38.7	−37.0	−37.6	−36.7	−1.3
ES0066	−35.0	−34.7	−37.7		−36.5	−35.0	−1.9
ES0068	−35.3	−34.9	−39.0	−37.1	−37.7	−37.1	−1.3
ES0080	−34.4	−33.8	−37.3	−35.4	−36.4	−35.0	−1.7
ES0083	−34.6	−34.4		−36.1	−37.1	−37.0	−0.6
ES0087	−35.2	−34.5	−38.6	−37.6	−37.4	−37.4	−0.5
ES0089	−35.3	−34.7	−38.1	−37.1	−37.5	−36.9	−0.8
ES0091	−35.4	−34.9	−38.1	−37.0	−36.9	−36.9	−0.5

carbon isotopic composition of isoprenoids (Pr and Ph) and provides a direct measure of this phenomenon (Table 5). That the isotopic order of these compound classes in pre-Ediacaran to early Ediacaran aged samples is opposite to that expected from biosynthetic relationships in photosynthetic organisms (Hayes, 2001; Schouten et al., 2008), was previously reported for bitumens from Australia and interpreted as signifying a fundamental re-organization of biogeochemical cycles at the close of the Proterozoic Eon (Logan et al., 1995, 1997). At the time of these studies, it was proposed that the isotopic ordering anomaly reflected intense heterotrophic reworking of organic matter in a redox-stratified ocean (Logan et al., 1995), while 'normal isotopic ordering' was characteristic of a ventilated water column. These authors also proposed that burial of organic matter in rapidly sinking fecal pellets instigated the change from the former state to the latter. While this hypothesis has been questioned, as macrozooplankton with sufficiently large fecal pellets likely evolved around 520 Ma (Chen and Zhou, 1997; Vannier and Chen, 2000; Peterson et al., 2005), changes in the isotopic ordering of isoprenoidal and acetogenic lipids may still be diagnostic of different ocean redox states and/or trophic regimes (Logan et al., 1995; Rothman et al., 2003; Fike et al., 2006; Butterfield, 2007). Further discussion of this topic is beyond the scope of the present report and will be treated in a separate paper.

4.4. Oil family analysis and age of the samples

The results of hierarchical cluster analyses of the MRM derived biomarker parameters presented in Tables 2 and 4, together with bulk $\delta^{13}C$ data for the saturate and aromatic hydrocarbons are presented in Fig. 8. The clustering follows closely the geographic and geochemical distinctions discussed above. Baykit High oils form a distinct group although sample ES0020 appears as a complete outlier. This particular oil is different in large part due to its anomalous steroid composition including a higher sterane/hopane ratio, a higher proportion of C_{27} steranes and lower abundances of 24-isopropylcholestanes. The other samples form two distinct clusters and this also correlates, to some extent, with geographical placement and, possibly, source sedimentary facies. Four of the oils in the smaller cluster (ES0022, ES0024, ES0026 and ES0035) are expected to be very similar as they are from the nearby Sobin and Paygin fields and reservoired in the Upper Vendian Vanavara Formation of the Katanga Saddle. Here, the sedimentary package is geographically, structurally and lithologically distinct from the coeval sequence of sedimentary rocks to the east in the Nepa-Botuoba Basin (Kochnev, 2008). The oil ES0043, although from the Nepa-Botuoba Basin, is reservoired in the Parshino Formation which correlates to upper sub-formations of the Vanavara Formation. The oils in the largest cluster mostly comprise samples from slightly younger reservoirs in the latest Vendian to Early Cambrian part of the Nepa-Botuoba sedimentary sequence. Similar results are obtained using GeoMark OilMod parameters (Zumberge et al., 2005) derived from SIM GC–MS, confirming the robustness of the geochemical distinctiveness of the two types of petroleum.

A paucity of precise radiometric ages and absence of oil-source correlations prevents placing any tight constraints on the ages of the sediments from which these oils originated. Given the known age distributions of sedimentary sequences across the eastern Siberia Platform, Ediacaran to Cambrian aged rocks appear to have sourced the oils of the Nepa-Botuoba and Katanga Saddle oils, with the Baykit High coming from Cryogenian age rocks. Obviously, these are very broad time windows. A microfossil assemblage in the upper Vanavara Formation of the Katanga Saddle has been correlated with acritarchs of the Pertatataka Formation in the Amadeus Basin (Australia), allowing its placement as 'basal upper Vendian' in the Russian stratigraphic nomenclature and this corresponds to Middle Ediacaran on the international stratigraphic scale (Chumakov and Semikhatov, 1981; Knoll et al., 2004). Oils reservoired in the Vanavara Formation are then likely to be Ediacaran, but not younger, and this assignment would be consistent with their close geochemical similarity to the Huqf oils of the SOSB. Huqf oils from within the Ara Evaporite sequence that encompasses the Ediacaran-Cambrian Boundary originate from rocks laid down 547–540 Ma (Bowring et al., 2007) are often *in situ*, that is,

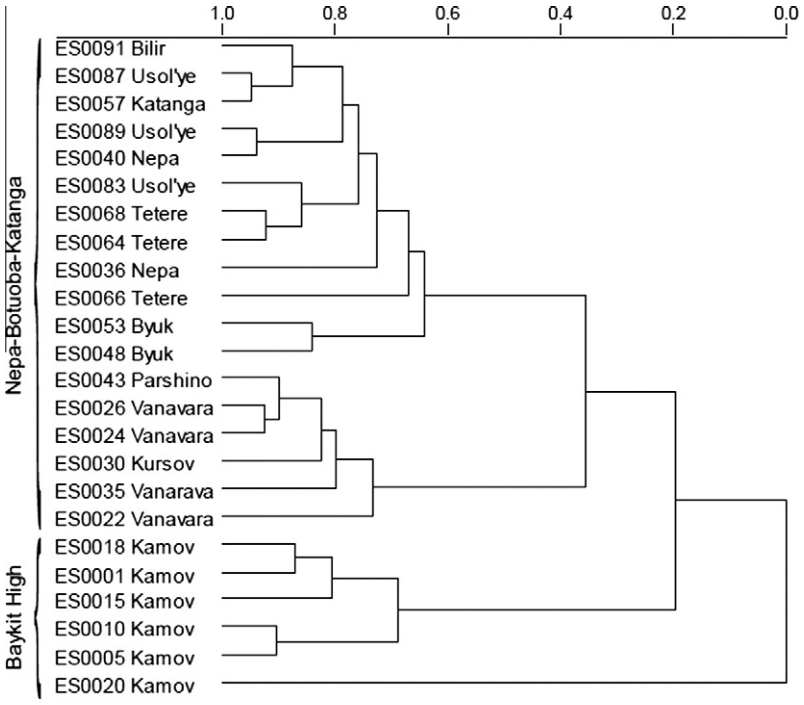

Fig. 8. Hierarchical cluster analysis showing the main oil families in the eastern Siberian oils. Variables used in this analysis are given in Tables 2, 4 and 5.

produced from carbonates, marls or silicilyte sediments that act both as source and reservoir (Grosjean et al., 2009). On the basis of geochemical data alone, the Katanga Saddle and Nepa-Botuoba oils probably come from rocks higher in the Ediacaran sequence (Ulmishek, 2001b).

Although the oils from the Baykit High are geochemically distinct, they are still very depleted in ^{13}C and have an abundance of steranes dominated by C_{29} homologues like other oils from eastern Siberia. This, combined with a high ratio of 24-isopropyl cholestanes/24-*n*-propylcholestanes, suggests they come from the upper part of the Precambrian sequence. By comparing microfossil assemblages and K-Ar and ^{40}Ar-^{39}Ar dating, the Kamov Group of the Baykit High has been suggested to be of Middle Riphean age with the uppermost section corresponding to the Late Riphean (1015–1030 Ma) (Frolov et al., 2011). Until the availability of precise radiometric ages improves and oils can be compared to potential source rocks, we cannot confidently assign an age to the source of these oils. Still, with the limited dating at hand combined with our geochemical parameters, it seems unlikely they are older than the Cryogenian and therefore do not originate from rocks >1050 Ma as has been suggested by Kontorovich et al. (1996).

5. Conclusions

In accordance with previous studies of eastern Siberian oils that examined Nepa-Botuoba oils, we report high relative abundances of X-peaks, a dominance of C_{29} steranes and C isotopic values that are significantly more depleted than for most oils known from the Phanerozoic (Fowler and Douglas, 1987; Summons and Powell, 1992). Similar properties have been reported for Late Precambrian oils from Oman (Grantham et al., 1988), the eastern European Platform (Bazhenova and Arefiev, 1996) and from India (Peters et al., 1995). In the present investigation, oils from the Nepa-Botuoba High and nearby Katanga Saddle are shown to be genetically similar to each other and to the Huqf oils of the SOSB (Grosjean et al., 2009). In particular, they share obvious signals of 24-isopropylcholestanes, which are derived from demosponges. They also show have acyclic isoprenoids (Pr and Ph) that are more enriched in ^{13}C than adjacently eluting C_{17} and C_{18} *n*-alkanes. They are distinct from the Huqf oils in having lower values for proxies that reflect water column salinity and stratification indicating that their source rocks, of probable Late Ediacaran to Early Cambrian age, were deposited under open marine conditions.

A second and geochemically distinct family of oils comes from Riphean sedimentary rocks on the Baykit High to the west of the Katanga Saddle. They are characterized by slightly higher Pr/Ph ratios, a lower abundance of steranes relative to hopanes, lower abundances of X-peaks and anomalous isotopic ordering where the acyclic isoprenoids Pr and Ph are more depleted than *n*-C_{17} and *n*-C_{18}. The majority of these oils also have appreciable contents of 24-isopropylcholestanes, which suggests that the oils are likely not older than Cryogenian in age. However, an outlier with very low 24-isopropylcholestane contents may indicate that a pre-Cryogenian source rock interval made variable contributions to these oils.

Acknowledgements

The authors acknowledge funding from the NSF-Biocomplexity Program EAR-0420592 and the NASA Astrobiology Institute to Roger Summons and Gordon Love. We also appreciate the award of a Linden Fellowship at MIT and research support from the National Italian American Foundation and The Tobacco Root Geological Society to Amy Kelly. We thank Carolyn Colonero for technical assistance and Simon George, Herbert Volk, and two anonymous reviewers for suggestions which improved the manuscript. Daniel Rothman, Andrew Knoll and Christopher Reddy provided valuable advice throughout this study.

Associate Editor – **Simon George**

References

Anbar, A.D., Knoll, A.H., 2002. Proterozoic ocean chemistry and evolution: a bioinorganic bridge? Science 297, 1137–1142.
Andrusevich, V.E., Engel, M.H., Zumberge, J.E., Brothers, L.A., 1998. Secular, episodic changes in stable carbon isotope composition of crude oils. Chemical Geology 152, 59–72.
Bazhenova, O.K., Arefiev, O.A., 1996. Geochemical peculiarities of Pre-Cambrian source rocks in the East European Platform. Organic Geochemistry 25, 341–351.
Bowring, S., Myrow, P., Landing, E., Ramezani, J., 2003. Geochronological constraints on terminal Neoproterozoic events and the rise of metazoans. Geophysical Research Abstracts 5, 219.
Bowring, S.A., Grotzinger, J.P., Condon, D.J., Ramezani, J., Newall, M., 2007. Geochronologic constraints on the chronostratigraphic framework of the Neoproterozoic Huqf Supergroup, Sultanate of Oman. American Journal of Science 307, 1097–1145.
Bristow, T.F., Kennedy, M.J., 2008. Carbon isotope excursions and the oxidant budget of the Ediacaran atmosphere and ocean. Geology 36, 863–866.
Butterfield, N.J., 2007. Macroevolution and macroecology through deep time. Palaeontology 50, 41–55.
Canfield, D.E., 1998. A new model for Proterozoic ocean chemistry. Nature 396, 450–453.
Canfield, D.E., Teske, A., 1996. Late Proterozoic rise in atmospheric oxygen concentration inferred from phylogenetic and sulphur-isotope studies. Nature 382, 127–132.
Chen, J., Zhou, G.-Q., 1997. Biology of the Chenjiang fauna. In: Chen, J., Cheng, Y.N., Iten, H.V. (Eds.), The Cambrian Explosion and the Fossil Record, Bulletin of the National Museum of Natural Science, vol. 10, Taichung, pp. 11–105.
Chumakov, N.M., Semikhatov, M.A., 1981. Riphean and Vendian of the USSR. Precambrian Research 15, 229–253.
Cloud Jr., P.E., 1968. Atmospheric and hydrospheric evolution on the primitive Earth: both secular accretion and biological and geochemical processes have affected earth's volatile envelope. Science 160, 729–736.
Collister, J.W., Summons, R.E., Lichtfouse, E., Hayes, J.M., 1992. An isotopic biogeochemical study of the Green River oil shale. Organic Geochemistry 19, 265–276.
Dahl, T.W., Hammarlund, E.U., Anbar, A.D., Bond, D.P.G., Gill, B.C., Gordon, G.W., Knoll, A.H., Nielsen, A.T., Schovsbo, N.H., Canfield, D.E., 2010. Devonian rise in atmospheric oxygen correlated to the radiations of terrestrial plants and large predatory fish. Proceedings of the National Academy of Sciences of the United States of America 107, 17911–17915.
Derry, L.A., 2010. On the significance of δ^{13} C correlations in ancient sediments. Earth and Planetary Science Letters 296, 497–501.
Des Marais, D.J., Strauss, H., Summons, R.E., Hayes, J.M., 1992. Carbon isotope evidence for the stepwise oxidation of the Proterozoic environment. Nature 359, 605–609.
Didyk, B.M., Simoneit, B.R.T., Brassell, S.C., Eglinton, G., 1978. Organic geochemical indicators of palaeoenvironmental conditions of sedimentation. Nature 272, 216–222.
Doughty, D.M., Hunter, R.C., Summons, R.E., Newman, D.K., 2009. 2-Methylhopanoids are maximally produced in akinetes of *Nostoc punctiforme*: geobiological implications. Geobiology 7, 524–532.
Everett, M.A., 2010. Characterizing the Precambrian petroleum systems of eastern Siberia: evidence from oil geochemistry and basin modeling. In: SPE Russian Oil and Gas Conference and Exhibition, 26–28 October 2010, Moscow, Russia, #136334-MS.
Farrimond, P., Talbot, H.M., Watson, D.F., Schulz, L.K., Wilhelms, A., 2004. Methylhopanoids: molecular indicators of ancient bacteria and a petroleum correlation tool. Geochimica et Cosmochimica Acta 68, 3873–3882.
Fike, D.A., Grotzinger, J.P., Pratt, L.M., Summons, R.E., 2006. Oxidation of the Ediacaran Ocean. Nature 444, 744–747.
Foster, C.B., Reed, J.D., Wicander, R., 1989. Gloeocapsomorpha prisca Zalessky, 1917: a new study. Part I: taxonomy, geochemistry, and paleoecology. Geobios 22, 735–759.
Fowler, M.G., Douglas, A.G., 1987. Saturated hydrocarbon biomarkers in oils of Late Precambrian age from Eastern Siberia. Organic Geochemistry 11, 201–213.
Frolov, S.V., Akhmanov, G.G., Kozlova, E.V., Krylov, O.V., Sitar, K.A., Galushkin, Y.I., 2011. Riphean basins of the central and western Siberian Platform. Marine and Petroleum Geology 28, 906–920.
Giddings, J.A., Wallace, M.W., Woon, E.M.S., 2009. Interglacial carbonates of the Cryogenian Umberatana Group, northern Flinders Ranges, South Australia. Australian Journal of Earth Sciences 56, 907–925.
Grantham, P.J., Lijmbach, J., Posthuma, J., Hughes Clarke, M.W., Willink, R.J., 1988. Origin of crude oils in Oman. Journal of Petroleum Geology 11, 61–88.

Grosjean, E., Love, G.D., Stalvies, C., Fike, D.A., Summons, R.E., 2009. New oil-source rock correlations in the South Oman Salt Basin. Organic Geochemistry 40, 87–110.

Harvey, H.R., McManus, G.B., 1991. Marine ciliates as a widespread source of tetrahymanol and hopan-3[beta]-ol in sediments. Geochimica et Cosmochimica Acta 55, 3387–3390.

Hayes, J.M., 2001. Fractionation of carbon and hydrogen isotopes in biosynthetic processes. Reviews in Mineralogy and Geochemistry 43, 225–277.

Hayes, J.M., Summons, R.E., Strauss, H., Des Marais, D.J., Lambert, I.B., 1992. Proterozoic biogeochemistry. In: Schopf, J.W., Klein, C. (Eds.), The Proterozoic Biosphere: A Multidisciplinary Study. Cambridge University Press, pp. 81–133.

Hoffmann, K.H., Condon, D.J., Bowring, S.A., Crowley, J.L., 2004. U-Pb zircon date from the Neoproterozoic Ghaub Formation, Namibia: constraints on Marinoan glaciation. Geology 32, 817–820.

Höld, I.M., Schouten, S., Jellema, J., Sinninghe Damsté, J.S., 1999. Origin of free and bound mid-chain methyl alkanes in oils, bitumens and kerogens of the marine, Infracambrian Huqf Formation (Oman). Organic Geochemistry 30, 1411–1428.

Kennedy, M., Droser, M., Mayer, L.M., Pevear, D., Mrofka, D., 2006. Late Precambrian oxygenation; inception of the clay mineral factory. Science 311, 1446–1449.

Klomp, U.C., 1986. The chemical structure of a pronounced series of iso-alkanes in South Oman crudes. Organic Geochemistry 10, 807–814.

Knoll, A.H., Carroll, S.B., 1999. Early animal evolution: emerging views from comparative biology and geology. Science 284, 2129–2137.

Knoll, A.H., Walter, M.R., Narbonne, G.M., Christie-Blick, N., 2004. A new period for the geologic time scale. Science 305, 621–622.

Knoll, A.H., Javaux, E.J., Hewitt, D., Cohen, P., 2006. Eukaryotic organisms in Proterozoic oceans. Philosophical Transactions of the Royal Society B 361, 1023–1038.

Knoll, A.H., Summons, R.E., Waldbauer, J., Zumberge, J., 2007. The geological succession of primary producers in the oceans. In: Falkowski, P., Knoll, A.H. (Eds.), The Evolution of Primary Producers in the Sea. Elsevier, Burlington, pp. 133–163.

Kochnev, B.B., 2008. Sedimentation settings of the Vendian Vanavara Formation, the Siberian platform. Stratigraphy and Geological Correlation 16, 20–30.

Kodner, R.B., Pearson, A., Summons, R.E., Knoll, A.H., 2008. Sterols in red and green algae: quantification, phylogeny, relevance for the interpretation of geologic steranes. Geobiology 6, 411–420.

Kontorovich, A.E., Izosimova, A.N., Kontorovich, A.A., Khabarov, E.M., Timoshina, I.D., 1996. Geologic framework and conditions of formation of the giant Yurubchen-Tokhom zone of oil and gas accumulation in the Upper Proterozoic of the Siberian craton. Geologiya i Geofizika 37, 166–195.

Li, C., Love, G.D., Lyons, T.W., Fike, D.A., Sessions, A.L., Chu, X., 2010. A stratified redox model for the Ediacaran ocean. Science 328, 80–83.

Logan, G.A., Calver, C.R., Gorjan, P., Summons, R.E., Hayes, J.M., Walter, M.R., 1999. Terminal Proterozoic mid-shelf benthic microbial mats in the Centralian Superbasin and their environmental significance. Geochimica et Cosmochimica Acta 63, 1345–1358.

Logan, G.A., Hayes, J.M., Hieshima, G.B., Summons, R.E., 1995. Terminal Proterozoic reorganization of biogeochemical cycles. Nature 376, 53–56.

Logan, G.A., Summons, R.E., Hayes, J.M., 1997. An isotopic biogeochemical study of neoproterozoic and early Cambrian sediments from the Centralian Superbasin, Australia. Geochimica et Cosmochimica Acta 61, 5391–5409.

Love, G.D., Grosjean, E., Stalvies, C., Fike, D.A., Grotzinger, J.P., Bradley, A.S., Kelly, A.E., Bhatia, M., Meredith, W., Snape, C.E., Bowring, S.A., Condon, D.J., Summons, R.E., 2009. Fossil steroids record the appearance of Demospongiae during the Cryogenian period. Nature 457, 718–721.

Love, G.D., Stalvies, C., Grosjean, E., Meredith, W., Snape, C.E., 2008. Analysis of molecular biomarkers covalently bound within Neoproterozoic sedimentary kerogen. In: Kelley, P.H., Bambach, R.K. (Eds.), Paleontological Society Papers, vol. 14. The Paleontological Society, pp. 67–83.

Luo, G., Xie, S., Wu, W., Sun, S., Huang, J., Shi, X., 2008. Molecular evidence for primary producers and paleo-environmental conditions in Mesoproterozoic in the Xuanlong depression in North China. Journal of China University of Geosciences 19, 567–576.

Macdonald, F.A., Schmitz, M.D., Crowley, J.L., Roots, C.F., Jones, D.S., Maloof, A.C., Strauss, J.V., Cohen, P.A., Johnston, D.T., Schrag, D.P., 2010. Calibrating the Cryogenian. Science 327, 1241–1243.

Maloof, A.C., Rose, C.V., Beach, R., Samuels, B.M., Calmet1, C.C., Erwin, D.H., Poirier, G.R., Yao, N., Simons, F.J., 2010. Possible animal-body fossils in pre-Marinoan limestones from South Australia. Nature Geoscience 3, 653–659.

McCaffrey, M.A., Moldowan, J.M., Lipton, P.A., Summons, R.E., Peters, K.E., Jeganathan, A., Watt, D.S., 1994. Paleoenvironmental implications of novel C_{30} steranes in Precambrian to Cenozoic Age petroleum and bitumen. Geochimica et Cosmochimica Acta 58, 529–532.

McFadden, K.A., Huang, J., Chu, X., Jiang, G., Kaufman, A.J., Zhou, C., Yuan, X., Xiao, S., 2008. Pulsed oxidation and biological evolution in the Ediacaran Doushantuo Formation. Proceedings of the National Academy of Sciences of the United States of America 105, 3197–3202.

Mel'nikov, N.V., Shabanov, Y.Y., Shabanova, O.S., 2010. Stratigraphic chart of Cambrian deposits in the Turukhansk-Irkutsk-Olekma region, Siberian Platform. Russian Geology and Geophysics 51, 672–683.

Moldowan, J.M., Seifert, W.K., Gallegos, E.J., 1985. Relationship between petroleum composition and depositional environment of petroleum source rocks. American Association of Petroleum Geologists Bulletin 69, 1255–1268.

Narbonne, G.M., 2005. The ediacarabiota: Neoproterozoic origin of animals and their ecosystems. Annual Review of Earth and Planetary Sciences 33, 421–442.

Peters, K.E., Clark, M.E., Das Gupta, U., McCaffrey, M.A., Lee, C.Y., 1995. Recognition of an Infracambrian source rock based on biomarkers in the Baghewala-1 oil, India. American Association of Petroleum Geologists Bulletin 79, 1481–1493.

Peters, K.E., Walters, C.C., Moldowan, J.M., 2005. The Biomarker Guide, second ed. Cambridge University Press, Cambridge.

Peterson, K.J., Butterfield, N.J., 2005. Origin of the Eumetazoa: testing ecological predictions of molecular clocks against the Proterozoic fossil record. Proceedings of the National Academy of Sciences of the United States of America 102, 9547–9552.

Peterson, K.J., Lyons, J.B., Nowak, K.S., Takacs, C.M., Wargo, M.J., McPeek, M.A., 2004. Estimating metazoan divergence times with a molecular clock. Proceedings of the National Academy of Sciences of the United States of America 101, 6536–6541.

Peterson, K.J., McPeek, M.A., Evans, D.A.D., 2005. Tempo and mode of early animal evolution: inferences from rocks, Hox, molecular clocks. Paleobiology 31, 36–55.

Powell, T.G., McKirdy, D.M., 1973. Relationship between ratio of pristane to phytane, crude oil composition and geological environment in Australia. Nature 243, 37–39.

Rashby, S.E., Sessions, A.L., Summons, R.E., Newman, D.K., 2007. Biosynthesis of 2-methylbacteriohopanepolyols by an anoxygenic phototroph. Proceedings of the National Academy of Sciences of the United States of America 104, 15099–15104.

Rothman, D.H., Hayes, J.M., Summons, R.E., 2003. Dynamics of the Neoproterozoic carbon cycle. Proceedings of the National Academy of Sciences of the United States of America 100, 8124–8129.

Rubinstein, I., Strausz, O.P., 1979. Geochemistry of the thiourea adduct fraction from an Alberta petroleum. Geochimica et Cosmochimica Acta 43, 1387–1392.

Scalan, E.S., Smith, J.E., 1970. An improved measure of the odd-even predominance in the normal alkanes of sediment extracts and petroleum. Geochimica et Cosmochimica Acta 34, 611–620.

Schouten, S., Özdirekcan, S., van der Meer, M.T.J., Blokker, P., Baas, M., Hayes, J.M., Sinninghe Damsté, J.S., 2008. Evidence for substantial intramolecular heterogeneity in the stable carbon isotopic composition of phytol in photoautotrophic organisms. Organic Geochemistry 39, 135–146.

Scott, C., Lyons, T.W., Bekker, A., Shen, Y., Poulton, S.W., Chu, X., Anbar, A.D., 2008. Tracing the stepwise oxygenation of the Proterozoic ocean. Nature 452, 456–459.

Seifert, W.K., Moldowan, J.M., 1980. The effect of thermal stress on source-rock quality as measured by hopane stereochemistry. Physics and Chemistry of the Earth 12, 229–237.

Seifert, W.K., Moldowan, M.J., 1978. Applications of steranes, terpanes and monoaromatics to the maturation, migration and source of crude oils. Geochimica et Cosmochimica Acta 42, 77–95.

Shiea, J., Brassell, S.C., Ward, D.M., 1990. Mid-chain branched mono- and dimethyl alkanes in hot spring cyanobacterial mats. A direct biogenic source for branched alkanes in ancient sediments? Organic Geochemistry 15, 223–231.

Sinninghe Damsté, J.S., Kenig, F., Koopmans, M.P., Köster, J., Schouten, S., Hayes, J.M., de Leeuw, J.W., 1995. Evidence for gammacerane as an indicator of water column stratification. Geochimica et Cosmochimica Acta 59, 1895–1900.

Sofer, Z., 1980. Preparation of carbon dioxide for stable carbon isotope analysis of petroleum fractions. Analytical Chemistry 52, 1389–1391.

Sofer, Z., 1984. Stable carbon isotope compositions of crude oils: application to source depositional environments and petroleum alteration. American Association of Petroleum Geologists Bulletin 68, 31–49.

Sokolov, B.S., Fedonkin, M.A., 1990. The Vendian System: Regional Geology. Springer-Verlag, Berlin, Heidelberg, New York.

Sperling, E.A., Pisani, D., Peterson, K.J., 2007. Poriferan paraphyly and its implications for Precambrian palaeobiology. Geological Society, London, Special Publications 286, 355–368.

Summons, R.E., Jahnke, L.L., Hope, J.M., Logan, G.A., 1999. 2-Methylhopanoids as biomarkers for cyanobacterial oxygenic photosynthesis. Nature 400, 554–556.

Summons, R.E., Powell, T.G., 1992. Hydrocarbon composition of the Late Proterozoic oils of the Siberian Platform: Implications for the depositional environment of the source rocks. In: Schidlowski, M., Golubic, S., Kimberley, M.M., McKirdy, D.M., Trudinger, P.A. (Eds.), Early Evolution and Mineral and Energy Resources. Springer Verlag, Berlin, pp. 296–307.

ten Haven, H.L., de Leeuw, J.W., Rullkötter, J., Sininnghe Damsté, J.S., 1987. Restricted utility of the pristane/phytane ratio as a palaeoenvironmental indicator. Nature 330, 641–643.

ten Haven, H.L., Rohmer, M., Rullkötter, J., Bisseret, P., 1989. Tetrahymanol, the most likely precursor of gammacerane, occurs ubiquitously in marine sediments. Geochimica et Cosmochimica Acta 53, 3073–3079.

Thiel, V., Jenisch, A., Wörheide, G., Löwenberg, A., Reitner, J., Michaelis, W., 1999. Mid-chain branched alkanoic acids from "living fossil" demosponges: a link to ancient sedimentary lipids? Organic Geochemistry 30, 1–14.

Ulmishek, G.F., 2001a. Petroleum geology and resources of the Baykit High province, East Siberia, Russia., U.S. Geological Survey Bulletin 2201-F.

Ulmishek, G.F., 2001b. Petroleum geology and resources of the Nepa-Botuoba High, Angara-Lena Terrace, Cis-Patom Foredeep, southeastern Siberian craton, Russia, US Geological Survey Bulletin 2201-C.

Van Waveren, I., Marcus, N., 1993. Morphology of recent copepod egg-envelopes from Turkey Point (Gulf of Mexico) and their implications for acritarch affinity. Special Papers in Palaeontology 48, 111–124.

Vannier, J., Chen, J.-Y., 2000. The Early Cambrian colonization of pelagic niches exemplified by *Isoxys* (Arthopoda). Lethaia 33, 295–311.

Volkman, J.K., Alexander, R., Kagi, R.I., Woodhouse, G.W., 1983. Demethylated hopanes in crude oils and their applications in petroleum geochemistry. Geochimica et Cosmochimica Acta 47, 785–794.

Welander, P.V., Coleman, M., Sessions, A.L., Summons, R.E., Newman, D.K., 2010. Identification of a methylase required for 2-methylhopanoid production and implications for the interpretation of sedimentary hopanes. Proceedings of the National Academy of Sciences of the United States of America 107, 8537–8542.

Yin, C.Y., Bengtson, S., Yue, Z., 2004. Silicified and phosphatized *Tianzhushania*, spheroidal microfossils of possible animal origin from the Neoproterozoic of South China. Acta Palaeontologica Polonica 49, 1–12.

Zumberge, J.E., Russell, J.A., Reid, S.A., 2005. Charging of Elk Hills reservoirs as determined by oil geochemistry. American Association of Petroleum Geologists Bulletin 89, 1347–1371.